PHASE DIFFERENCE MONITOR BETWEEN SUPERKEKB INJECTOR LINAC AND RINGS USING DIRECT SAMPLING TECHNIQUE

N. Liu[†,1], T. Miura[1,2], T. Matsumoto[1,2], F. Qiu[1,2], S. Michizono[1,2], D. Arakawa[2], H. Katagiri[2], Y. Yano[2], B.T. Du[1], [1]SOKENDAI, Kanagawa 240-0193, Japan, [2]KEK, Ibaraki 305-0801, Japan

Abstract

In the SuperKEKB Phase2 operation, the beam injection phase from the injector LINAC to rings drifts several degrees or more per day. The monitoring and compensation system of the phase drift between the LINAC master oscillator (MO) and the ring MO is important for stable beam injection. The frequency of LINAC MO and the ring MO is 571.2 MHz and 508.9 MHz, respectively. Both MO signals are monitored by the direct sampling technique using the same sampling frequency (clock). There are several combinations of the clock generation. In this paper, the possible three combinations will be compared including the clock jitter performance and the short-term phase stability and the combination 1 is selected for the phase difference monitor system. The 1ms short-term phase stability is 0.04 deg. (RMS) without digital filter and 0.005 deg. (RMS) with 10 kHz bandwidth digital filter for both MO signals in the laboratory. Finally, the long-term phase drift between LINAC MO and ring MO is monitored at the injector LINAC.

INTRODUCTION

The luminosity of the SuperKEKB upgrade project is 40 times higher than KEKB. The lower-emittance and higher-current beam is required. The beam injection phase stabilization between the injector LINAC to rings is very important for stable beam injection. Figure 1 shows the master oscillator (MO) system for LINAC, damping ring (DR) and main ring (MR). The MO of the LINAC and the rings is 571.2 MHz and 508.9 MHz, respectively. They are synchronized by 10 MHz trigger but the phase drift between them was found to be several degrees per day [1].

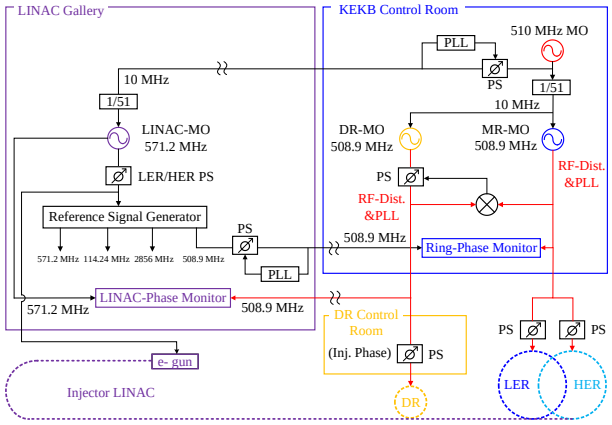

Figure 1: Master oscillator system for LINAC, damping ring and main ring.

† liuna@post.kek.jp

For the radio frequency (RF) phase detection in accelerators, the analog down-conversion with digital IQ (In-phase and Quadrature component) detection and direct sampling technique are widely used [2]. The direct sampling technique gets rid of the down-converter and makes the RF measurement circuit much simpler and smaller, but it is sensitive to the clock jitter [3]. In the direct sampling technique, all the frequency components within the ADC bandwidth are converted into the first Nyquist zone. The non-IQ algorithm can suppress the harmonics of the carrier frequency and digitally reduce the clock jitter induced measurement errors by averaging over multiply samples [4]. Therefore, the higher phase measurement accuracy can be achieved. The frequency of the measured RF signal is different so that the direct sampling technique is more suitable.

In this paper, we monitor the two MO signals with different frequency by the direct sampling technique using the same sampling frequency. The possible combinations of the clock generation for the phase monitor system will be compared including the clock jitter and short-term phase stability. The short-term phase stability is improved by applying the digital low pass filter (LPF). After the system performance evaluation, the phase difference monitor system is implemented at injector LINAC gallery and the long-term phase drift between two MOs is measured.

DIRECT SAMPLING AND NON-IQ DETECTION

The RF frequency can be measured with the sampling rate lower than the Nyquist rate (twice the maximum frequency component in the signal), which called the undersampling or direct sampling technique [5]. In order to derive the phase of the RF signal, the sampling frequency must be synchronized with the frequency of the measured RF signal and selected based in the non-IQ algorithm [3, 6]. The sampling frequency f_s and the measured RF frequency f_{RF} must satisfy

$$f_s = \frac{f_{RF}}{K + \frac{N}{M}}, \mathrm{K} = 0,1,2... \quad (1)$$

where N is an integer and M is also an integer but greater than 3, N and M represent the phase difference $\Delta\varphi$ between adjacent samples

$$\Delta\varphi = \frac{N}{M} \bullet 2\pi \quad (2)$$

The I and Q baseband component of the sampled RF signal can be calculated by the following equations

$$I = \frac{2}{M}\sum_{n=0}^{M-1} x[n]\sin\left(\frac{N}{M}\bullet 2\pi \bullet n\right) \quad (3)$$

$$Q = \frac{2}{M}\sum_{n=0}^{M-1} x[n]\cos\left(\frac{N}{M}\bullet 2\pi \bullet n\right) \quad (4)$$

where $x[n]$ is the n^{th} ADC sampled data. The phase (φ) of the measured RF signal can be calculated by $\varphi = \tan^{-1}(Q/I)$. Hence, the phase of the RF signal is obtained.

SELECTION AND GENERATION OF THE SAMPLING FREQUENCY

The numerical relationship between LINAC MO (571.2 MHz) and ring MO (508.9 MHz) is

$$\frac{f_{LINAC\_MO}}{f_{RING\_MO}} = \frac{571.2MHz}{508.9MHz} = \frac{55}{49}$$

In order to sample two different frequency MO signals by the same sampling frequency, the K, M and N coefficients must satisfy the following formula from Eq. (1)

$$f_s = \frac{f_{LINAC\_MO}}{K_1 + \frac{N_1}{M_1}} = \frac{f_{RING\_MO}}{K_2 + \frac{N_2}{M_2}} \text{ , and } M_1 = M_2 = M$$

So $K_1M + N_1 = 55$ and $K_2M + N_2 = 49$.

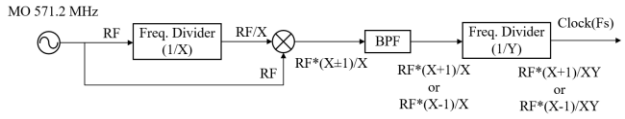

Figure 2: Block diagram of the clock generation for direct sampling technique.

Table 1: Possible Combinations of Sampling Frequency

Combination	X		Filter [MHz]	Y	Clock [MHz]	*M*
1	11	+	623.13	5	124.63	12
×	11	-	519.27	5	103.85	10
2	5	+	685.44	11	62.31	6
3	5	-	456.96	11	41.54	4

The block diagram of the clock generation for direct sampling is shown in Fig. 2 [7]. The LINAC MO 571.2 MHz is used as MO for clock generation. The frequency of 571.2 MHz MO signal (RF) is divided by X and then mix with itself to obtain another frequency $RF \bullet (1 \pm 1/X)$. Then this frequency is filtered by a band pass filter (BPF) or LPF. Finally, the filtered signal is divided by Y with another frequency divider to generate the required sampling frequency. The sampling frequency can be calculated by the following equation

$$f_s = \frac{f_{LINAC\_MO}}{\frac{XY}{X \pm 1}} \quad (5)$$

Where X, Y are both integers. Therefore, $K_1M + N_1 = XY = 55$ and $M = X \pm 1$.

The possible combinations (comb.) of sampling frequency for LINAC MO (571.2 MHz) is summarized in Table 1. The combination of $M = 10$ and $N_1 = 5$ can't provide enough amplitude and phase information of the measured RF signal. So the other three combinations are considered.

SYSTEM PERFORMANCE EVALUATION

Measurement setup

The configuration of the clock generation and the phase difference monitor system by direct sampling technique is shown in Fig. 3. The 571.2 MHz MO signal is generated by the signal generator (Keysight E8663D) and then split in two. One is used to generate the 571.2 MHz (LINAC MO frequency) signal and 508.9 MHz signal (ring MO frequency), the other is for the clock generation. The 571.2 MHz signal and 508.9 MHz signal are sampled by ADC1 and ADC2 (14-bit, 400 MSPS ADS5474), individually. According to the different RF frequency, different pairs of N_1, M_1 and N_2, M_2 are applied to non-IQ algorithm based on the same sampling frequency and then the IQ components are calculated inside field programmable gate array (FPGA) board. The phase of each RF signal is obtained and the phase difference between 571.2 MHz signal and 508.9 MHz signal is monitored.

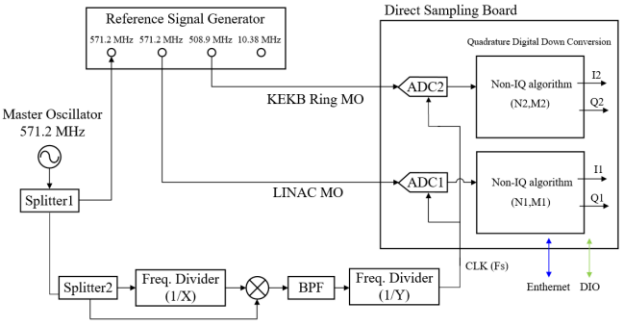

Figure 3: Configuration of the clock generation and the phase monitor system by direct sampling technique.

Jitter performance of the clock signal

In direct sampling technique, the measurement error is sensitive to the clock jitter. The RMS jitter of the clock signals generated by three combinations (Comb.) are measured by the signal source analyzer from 10 Hz to 10 MHz. Figure 4 shows the single side-band phase noise power spectrum of three clock signals. Table 2 summarizes the results of the clock jitter. The combination 1 has the best jitter performance.

Table 2: RMS Jitter and Phase Noise for Clock Signals

	Freq. [MHz]	Power [dBm]	Jitter [fs]	Phase Noise [mdeg.]
Comb.1	124.63	-2.58	126.48	5.67
Comb.2	62.31	-3.36	222.23	4.99
Comb.3	41.54	-1.88	464.7	6.95

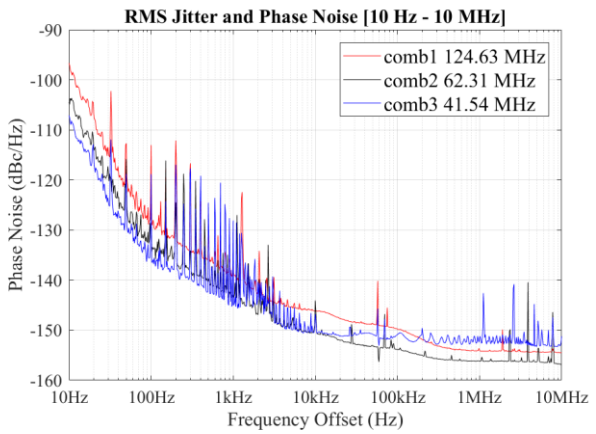

Figure 4: Jitter performance of the clock signals.

Short-term stability

In order to compare the short-term stability in time domain, the phase stability of two different RF signals (571.2 MHz and 508.9 MHz) sampled by three different sampling frequencies is measured by the phase difference monitor system as shown in Fig. 2. The coefficients (N_1 , N_2 , M) of the non-IQ algorithm for 571.2 MHz signal and 508.9 MHz signal are listed in Table 3, respectively.

Table 3: Coefficients of Non-IQ Algorithm

Combination	Clock [MHz]	M	N_1	N_2
1	124.63	12	7	1
2	62.31	6	1	1
3	41.54	4	3	1

Table 4: 1ms Short-term Phase Stability in Deg. (RMS)

Combination	571.2 MHz	508.9 MHz
1	0.038	0.035
2	0.058	0.054
3	0.081	0.086

Table 4 summarizes the 1ms short-term phase stability of three combinations without digital filter in degree (RMS). The combination 1 has the best performance in short-term stability due to the low clock jitter and the averaging over many multiply samples. The phase stability of 571.2 MHz and 508.9 MHz RF signals is 0.038 deg. RMS and 0.035 deg. RMS, respectively. So the combination 1 is selected for the phase difference monitor system between SuperKEKB injector LINAC MO and ring MO.

For the phase difference monitor system, the target is to measure the long-term phase drift between LINAC MO and ring MO. For higher accuracy, the IQ components of the RF signals are filtered by the digital infinite impulse response (IIR) LPF to suppress the clock jitter and ADC noise [8]. The 1ms short-term phase stability of the combination 1 without and with different bandwidth IIR LPF is shown in Fig. 5. The phase stability is up to 0.005 deg. RMS with 10 kHz bandwidth IIR LPF.

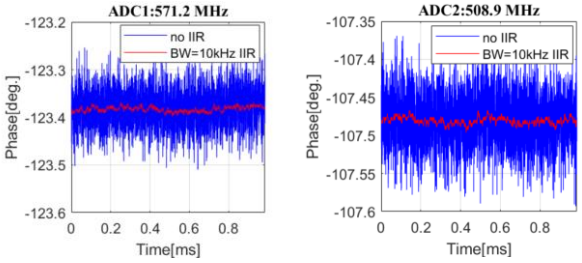

Figure 5: The 1ms short-term phase stability of the combination 1 for 571.2 MHz (left) and 508.9 MHz (right) MO signals without IIR LPF (blue line) and with 10 kHz bandwidth (BW) (red line) IIR LPF.

SHORT-TERM AND LONG-TERM MEASUREMENT RESULT AT LINAC

Jitter performance

The phase noise is measured by the signal source analyser from 10 Hz to 10 MHz. Figure 6 shows the single side-band phase noise power spectrum of MO signals and the clock signal. The RMS jitter is 97.32 fs (LINAC MO), 104.78 fs (LINAC MO monitored signal), 172.48 fs (ring MO monitored signal) and 167.54 fs (clock signal).

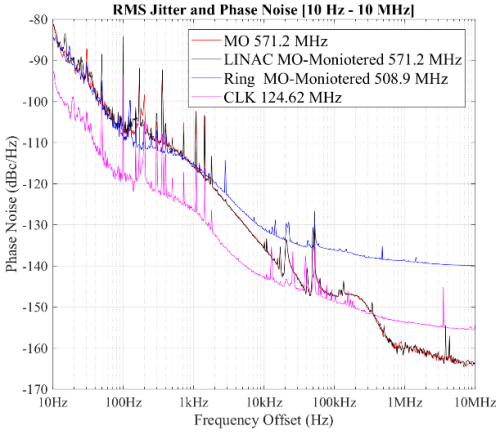

Figure 6: Single side-band phase noise power spectrum from 10 Hz to 10 MHz for MO signals and clock signal.

Long-term phase drift

The LINAC MO signal and ring MO signal are monitored by the phase difference monitor system by direct sampling technique with the sampling frequency 124.62 MHz. Both IQ data is filtered by 10 kHz IIR LPF for higher accuracy. Then the averaged raw data is used for the long-term phase drift measurement. All the monitor system is inside the thermostat chamber to minimize the system phase drift. The phase drift between LINAC MO and ring MO is observed 2.3 deg. (peak to peak) for 2 days by the phase difference monitor at LINAC (blue line) in Fig. 7.

The phase difference is also monitored by the phase monitor at rings. The results are matched very well as shown in Fig. 7. The phase drift compensation system is under consideration for stable beam injection.

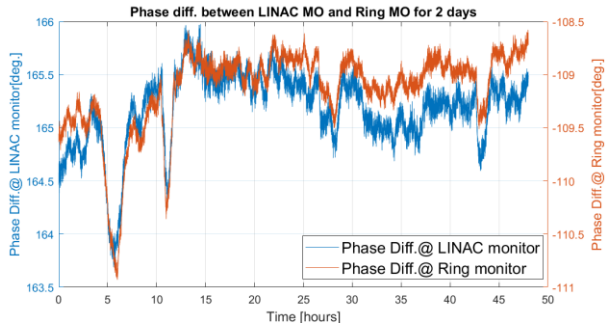

Figure 7: The long-term phase drift of the phase difference between LINAC MO 571.2 MHz (ADC1) and ring MO 508.9 MHz (ADC2) with 10 kHz bandwidth IIR LPF. The blue line is monitored by the phase monitor at LINAC and the orange line is monitored by the phase monitor at rings.

CONCLUSION

In order to monitor the different frequency 571.2 MHz and 508.9 MHz RF signals by the direct sampling technique using the same sampling frequency, the performance of the three possible combinations of the clock generation are evaluated in the laboratory including the clock jitter and short-term phase stability. The combination 1 of the clock generation is selected due to its good jitter performance and short-term stability. The clock jitter of combination 1 is 126.48 fs at 124.63 MHz and the 1ms short-term phase stability is 0.04 deg. (RMS) without digital filter. The short-term phase stability is improved by applying the digital IIR LPF for higher accuracy and the phase stability is up to 0.005 deg. (RMS) with 10 kHz bandwidth IIR LPF for both MO signals. Finally, the phase different monitor system is implemented based on the combination 1 at injector LINAC gallery. SuperKEKB LINAC MO signal (571.2 MHz) and ring MO signal (508.9 MHz) are both monitored at LINAC and rings and the results are well matched. The long-term phase drift between two MOs is observed 2.3 deg. for 2 days. The phase drift compensation system is under consideration for stable beam injection.

REFERENCES

[1] T. Kobayashi *et al.*, "LLRF control and master oscillator system for damping ring at SuperKEKB", in *Proc. IPAC'18*, Vancouver, BC, Canada, 2018, paper WEPAL001.

[2] T. Schilcher, "RF applications in digital signal processing", in *Proc.CAS–CERN Accelerator School: Course on Digital Signal Processing*, D. Brandt, Ed. Geneva, Switzerland: CERN, 2008, pp. 249–283.

[3] Z. Geng, S. N. Simrock, "Evaluation of fast ADCs for direct sampling RF filed detection for the European XFEL and ILC", in *Proc. LINAC'08*, Victoria, BC, Canada, 2008, paper THP102, pp. 1030-1032.

[4] S. Jablonski *et al.*, "2π low drift phase detector for high-precision measurements", *IEEE transactions on nuclear science*, vol. 62, NO. 3, Jun. 2015.

[5] P. Poshala, "Why Oversample when undersampling can do the job?", Texas Instruments, Dallas, TX, USA, Application Rep. SLAA594A, Jul. 2013

[6] M. Grecki, T. Jezynski, and A. Brandt, "Estimation of IQ vector components of RF field–theory and implementation," in *Proc. 12th Mixed Design of Integrated Circuits and Systems (MIXDES)*, Cracow, Poland, 2005, pp. 783–788.

[7] T. Matsumoto *et al.*, "Simultaneous measurement of RF signal and LO signal using direct sampling detection technique", in *Proc. 14th Annual Meeting of the Japanese Society of accelerator (PASJ'17)*, Hokkaido, Japan, Aug. 2017, paper TUP063, pp. 493-495.

[8] F. Qiu, private communication, July 2018.